We are IntechOpen, the world's leading publisher of Open Access books Built by scientists, for scientists

6,900
Open access books available

185,000
International authors and editors

200M
Downloads

Our authors are among the

154
Countries delivered to

TOP 1%
most cited scientists

12.2%
Contributors from top 500 universities

WEB OF SCIENCE™

Selection of our books indexed in the Book Citation Index in Web of Science™ Core Collection (BKCI)

Interested in publishing with us?
Contact book.department@intechopen.com

Numbers displayed above are based on latest data collected.
For more information visit www.intechopen.com

Chapter 5

Active Compact Antenna for Broadband Applications

Y. Taachouche, M. Abdallah, F. Colombel,
G. Le Ray and M. Himdi

Additional information is available at the end of the chapter

http://dx.doi.org/10.5772/58839

1. Introduction

The recent development of wireless communication technology and the miniaturization of electronics components increase the demand for compact systems applications including small antennas. One of the major challenges is the integration of antennas inside devices in a limited area. The main characteristics of these antennas are large frequency bandwidth and small size.

Many passive antennas such as monopole, dipole and printed antenna have been largely studied to yield small size relatively to the wavelength or broadband behavior. Previous studies have shown that antenna miniaturization impacts negatively antenna bandwidth and impedance matching [1].

The active antennas have found a wide interest for industrial applications in last years. The terminology of the active antenna indicates that the passive antenna elements are combined with an active device on the same substrate to provide a non-separated device and to improve antenna performances, especially in the field of size reduction and frequency bandwidth. The ability to adjust the size reduction and the frequency bandwidth of an active antenna is also very suitable when the antenna is included inside devices with many components located in a limited area.

In this chapter, we are interested in the improvements brought by the active antennas towards size reduction and the covered bandwidth. We present our work on compacts actives antennas in which we develop new techniques to reduce the size of antennas with good performances. Our main works is carried on two solutions; the first one is a broadband antenna with a very important size reduction. This solution corresponds to an active printed monopole integrating a bipolar transistor directly on the antenna structure without matching circuit. The second solution is a tunable narrow frequency band antenna operating on a wide band based on a printed loop antenna associated to a varactor diode.

INTECH
open science | open minds

© 2014 The Author(s). Licensee InTech. This chapter is distributed under the terms of the Creative Commons Attribution License (http://creativecommons.org/licenses/by/3.0), which permits unrestricted use, distribution, and reproduction in any medium, provided the original work is properly cited.

2. Active monopole antenna

2.1. Introduction

Miniaturized and broadband antennas with ominidirectional coverage have attracted attention for industrial applications. For example, today's mobile phones are innovative devices that provide a wide variety of services to users. One of the most attractive mobile phone services is the entertainment services, and especially the functionality that allows users to listen to FM radios through their mobile phones. This development induces a growing demand of FM antennas for mobile phones, and the necessity of innovative technologies to develop internal small FM antennas, which replace the external wire antennas that exhibit current mobile phones in the market. For automobile application, many radio systems as communication system, FM radio reception are collocated on the top roof of the car, and the very low visual impact of the antenna is required. The goal of this section is to propose a compact antenna to replace the historical monopole to improve the integration capability of the antenna in VHF band applications systems.

The idea of using active antennas can be traced back to as early as 1928 [2]. A small antenna with electron tube was commonly used in radio broadcast receivers around 1MHz (Figure 1).

With the invention of high frequency transistor, the studies of active antennas have been performed in the years 60-70 [3-11].

Literature contribution on active antennas exhibits several advantages, the frequency bandwidth or signal to noise improvements compared to a passive antenna of the same size. In this contribution, we have started from the results given by Meinke [4] who have inserted the electronic components (tunnel diode and transistor) directly on the structure without matching network.

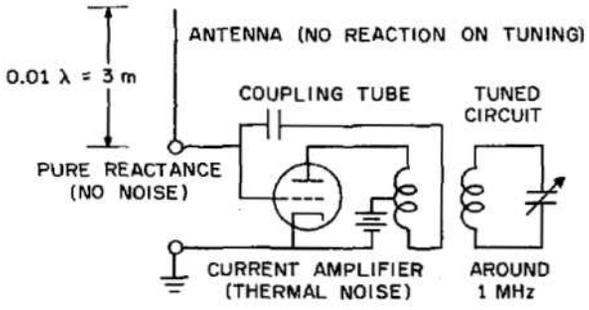

Figure 1. Active receiving antenna

A combination of a resonance half wavelength dipole with a VHF transistor has been proposed in [4]. The size of the antenna related to the wavelength is $\lambda/2$. As it is mentioned in [12], an active antenna provides new opportunities for many applications including the increase of bandwidth or the size reduction. In [13], a loop dipole has been proposed as a transmitting antenna. A total height of $\lambda/2000$ has been built and compared to a passive dipole which has

http://dx.doi.org/10.5772/58839

the same height. The active antenna is very broadband and operates at very low frequencies besides its very small size. In [14], it has been explained that an active monopole fed by a microwave transistor provides a wider frequency bandwidth than a passive monopole.

In order to provide innovative designs, the growing interest for active antennas has required more accurate analysis method. A hybrid analysis including electromagnetic full wave and nonlinear circuit solver is used in [15] and accurate theoretical results validated with measurements on an oscillator active antenna are provided. In [16], the analysis method used in a circuit voltages generated by a CAD software as source distribution for a magnetic current radiation calculation to allow estimation of the integrated antenna is presented. In [17], theoretical or experimental methods are explained to study active antennas.

In this section, the problem of matching a short monopole antenna by including a transistor in the monopole structure is presented. We are interested in the influence of the transistor on the behavior of active antenna towards size reduction, bandwidth and gain. We investigate an active receiving antenna based on a printed monopole associated to a bipolar transistor. In the first part, we will present the antenna design working on the VHF/UHF bands and the theoretical approach. In the second part, we will exhibit results for two transistor configuration. Measurement results will be compared to the simulated ones and the influence of the transistor location on the monopole will be studied.

2.2. Design of the active monopole antenna

The structure of the active receiving antenna is shown in Figure 2. The antenna is a combination of a monopole and a high frequency bipolar transistor (BFR182). The antenna has been printed on a Neltec NX9300 substrate (ε_r=3, h=0.786 mm, tanδ=0.0023) and is placed above a limited square reflector plane (500×500×4 mm^3). As shown in Figure 2, the monopole has been cut in to two parts and the bipolar transistor BFR 182 is directly integrated between these two parts of the monopole without matching circuit. The antenna is connected to a SMA connector through a 50 Ω microstrip line [18-19].

We separate the printed structure into two zones. The first one is the area on which the monopole is printed; the second region (Area 2) welcomes the elements of the bias circuit of the transistor. A printed line, called "parasite" is added to connect the third pin of the transistor to ground in area 2 at a distance p from the monopole.

The active component used in our work is a bipolar PNP transistor BFR 182 used for low noise and high-gain broadband amplifier applications, and operates up to 8GHz. The transistor is located at h_2 over the ground plane and is used in two configurations. The first one is the common emitter configuration. In this case, the emitter of the transistor is grounded through the parasitic printed line, the transistor base and collector are respectively linked to the upper part and to the bottom part of the monopole.

The second one is the common collector configuration, the base of the transistor is connected to the upper part and the emitter of the transistor to the lower part of the monopole, the collector is connected to ground via the parasite line.

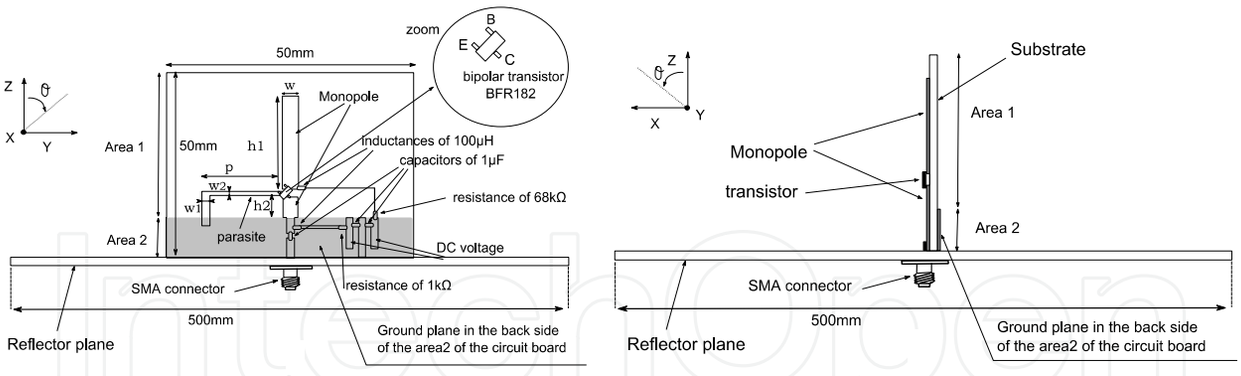

(a) Front view (b) Side view

(h_1=25mm, h_2=5mm, p=20mm, w=4mm, w_1=2mm, w_2=1mm)

Figure 2. Geometry of the proposed active receiving antenna

When V_{CC}=18V and V_{BB}=8.3V, the transistor is biased with I_C=10mA and V_{CE}=8V for common emitter configuration, I_C=4.8mA and V_{CE}=4.86V for common collector configuration. The resistances values (R_1=1kΩ, R_2=68kΩ) have been calculated in order to obtain the collector to emitter voltage (*Vce*) and collector current (*Ic)* required.

2.3. Calculation methods

We present here the theoretical and experimental methods of calculation used to evaluate the performance of the active monopole antenna. There are several methods to simulate and calculate the performance of an active antenna. Our choice is based on the method of combining the results of the electromagnetic calculation of the antenna structure with electrical model of the bipolar transistor. It conducts to a full analysis of the active antenna. This simulation was performed with CST Microwave Studio®.

With this method, only the input impedance of the active receiving antenna is calculated, because the antenna operates only at the reception due to unilaterally of the transistor. Hence, it is impossible to calculate the radiation characteristics (pattern, gain) with the usual calculate methods.

To solve this problem, we calculate the gain of the active receiving antenna by using the Link Budget method explained in [17], the setup system is illustrated in the Figure 3.

We compute the transmission parameter between a transmitting reference antenna and the active receiving antenna separated by the distance D.

Then by using the FRIIS formula (1) and knowing G_i, the transmitter antenna gain (2.1dBi), we are able to deduce G_r the gain of the active antenna.

$$S_{21} = Gi + Gr + 20 \log \left(\lambda / 4\pi D\right) \quad (1)$$

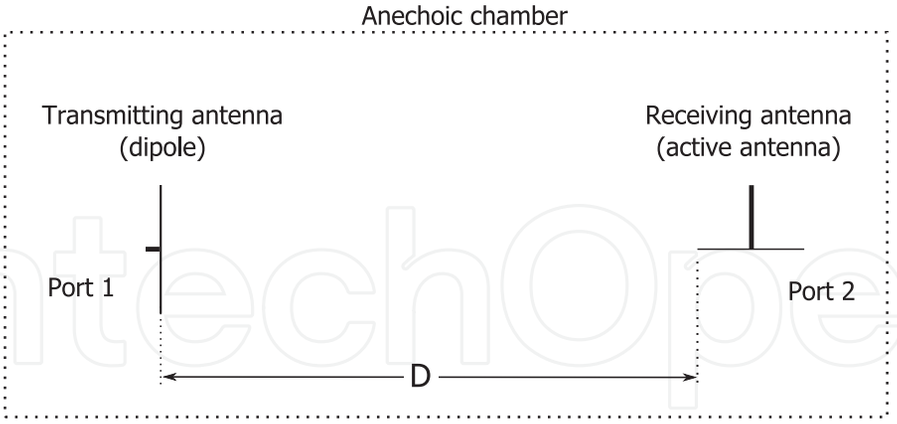

Figure 3. Two-port system proposed to calculate the active antenna performances.

Where *Gi* is the transmitter antenna gain, *Gr* the receiver antenna gain and D the distance between the two antennas. To ensure the validity of formula (1), the distance between the antennas (D) must satisfy the far field condition and the antennas are matched to 50Ω.

2.4. Theoretical results and measurements

Despite the difficulty to simulate an active antenna, we use CST software to achieve consistency between measurements and simulations. Several parameters, as the position of the transistor, the position of the parasite and the design of the antenna are investigated. All of these parameters allow us to vary the impedance of the active antenna and adjust the frequency band. In this section, we present theoretical and experimental results obtained on the active receiving antenna which operates in VHF band.

The antenna presented is working on the FM band (88-108MHz). We investigate the influence of the integration of the transistor in the monopole without matching circuit, its impact on the input impedance, and the size reduction.

We start with the influence of the height of the active monopole antenna (h_1) on its resonance frequency. Then, we investigate the influence of the transistor location on the monopole (h_2) and the position of the parasitic line (p) both on the return loss and on the gain through the calculation of the S_{21} (formula. 1) in both configurations.

2.4.1. Influence of the height of antenna

In this section, we present the theorical results of the performance of the active receiving antenna versus the height of the monopole (h_1), the transistor is positioned at $h_2=h_1/2$ (Figure 4). The heights of the active monopole (h_1) vary between 355 mm and 30 mm.

The theoretical results of the return loss of the active monopole as function of h_1 for both configurations, common emitter and common collector are shown in Figure 5.

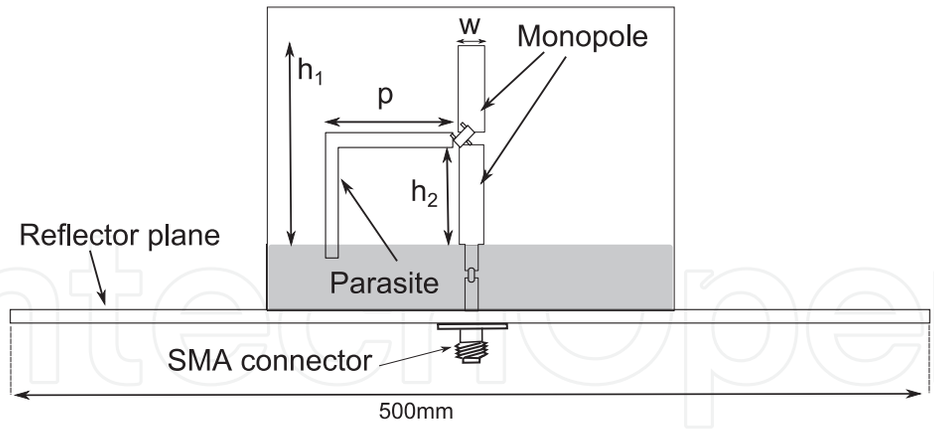

Figure 4. Geometry of the active monopole antenna.

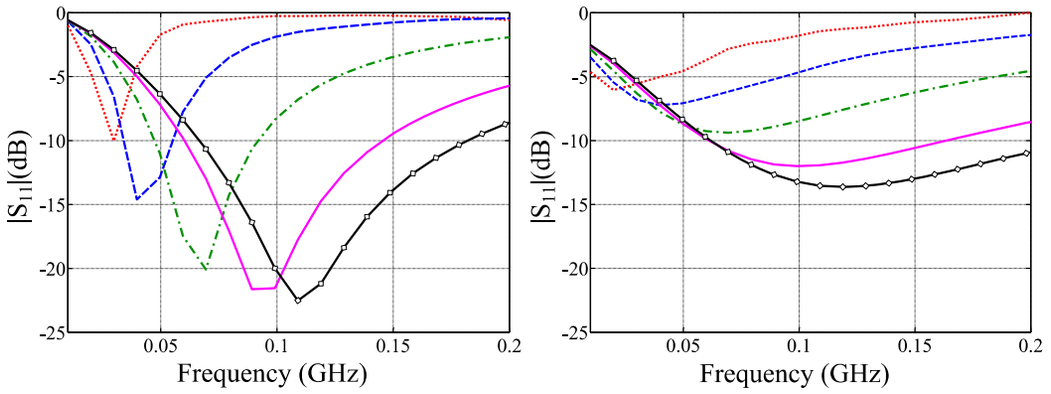

(···h_1=355mm, – – –h_1=177mm,-·-·-h_1=88mm, ——h_1=44mm, –▫– h_1=30mm)

Figure 5. Return loss of the active receiving antenna as function of the h_1. (a) Common emitter configuration, (b) Common collector configuration

As a result, we note a very low resonance frequency of active monopole. This resonance frequency depends on the height of the monopole and the configuration of the transistor used.

For the common-emitter configuration, the reduction factor is $\lambda/34$ for h_1=355 mm with a resonance frequency of 25 MHz and it is $\lambda/92$ for h_1=30mm with a resonance at 109 MHz. We also note that the resonance frequency of the active monopole does not vary linearly versus the length of the antenna as a liability for classical monopole. In our case, every time the height of the monopole is halved, the resonance frequency is multiplied by a coefficient which varies between 1.4 and 1.6. For the common collector configuration, we have a reduction factor of $\lambda/42$ for h_1=355mm and $\lambda/83$ for h_1=30mm.

We summarize in Table 1 the matching frequencies obtained for different heights of the active monopole for common emitter and common collector configurations.

h_1 (mm)	Emitter common configuration		collector common configuration	
	Fr (MHz)	Reduction ratio(λ/ h_1)	Fr (MHz)	Reduction ratio(λ/ h_1)
355	25	34	20	42
177	45	38	40	42
88	65	52.5	70	48
44	94	72.5	100	68
30	109	92	120	83

Table 1. Matching frequencies of the active monopole and size reduction ratio as function of the height h_1

This study provides the first results that we can suggest for reducing the active antennas size. In this first part, the transistor is placed at mid-height of the active monopole. To provide an accurate justification of the influence of the transistor on the miniaturization of the antenna, we will study in the next sub-section the influence of the position of the transistor on active monopole (influence of height h_2).

2.4.2. Influence of the position of the transistor

In this paragraph, we set the height of the active monopole antenna h_1 to 30 mm. We investigate the influence of the transistor location on the monopole (h_2) both on the return loss and the gain through the calculation of the S_{21}. We present the theoretical and experimental results for three different locations. The measurement process was performed in an anechoic chamber and the reference transmitting antenna was a telescopic dipole TR1722. The distance between the two antennas is 4.7m.

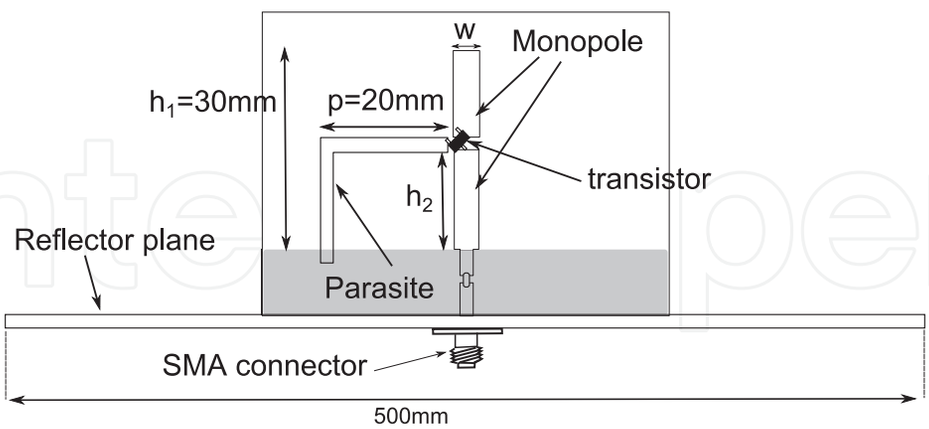

Figure 6. Position of the transistor on the active receiving antenna

2.4.2.1. Input impedance and gain

a. Common emitter configuration

The adaptation of the active antenna could be evaluated by the reflection coefficient at the output (S_{22}) of the two-port system described in Figure 3.

In Figure 7, the simulated and the measured $|S_{22}|$ are plotted for three transistor locations (h_2). Even if there is a shift between theories and measurements, the results are still in good agreement. These discrepancies are probably due to the difference between the theoretical parameters of the transistor provided by the PSPICE model and the real one. It can be noticed that the frequency bandwidth increases when the transistor is located close to the ground plane (h_2=5mm). The measurements exhibit a-10dB bandwidth of 77% around 77MHz when the transistor is located 25mm over the ground plane and 94% around 107.5MHz when the transistor is placed 5mm over the ground plane. In the first case (h_2=25mm) the height of the active antenna is close to $\lambda/212$ at the lowest operating frequency and when h_2=5mm the height of the monopole is $\lambda/175$.

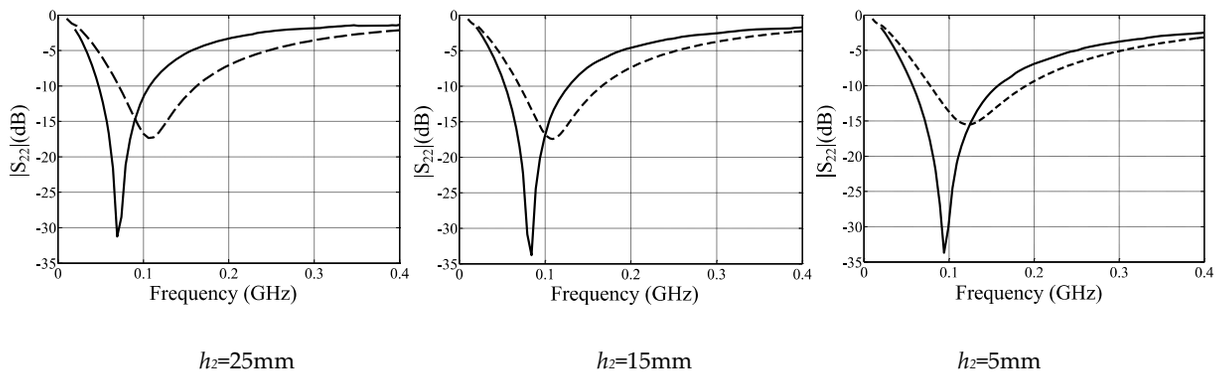

Figure 7. $|S_{22}|$ of the active receiving antenna an common emitter configuration (— measurement,---simulation)

We summarized the simulated and the measured frequency bandwidth results of the active receiving antenna in the Table 2.

For the gain of the active receiving antenna, we present the simulated and measured results of the transmission coefficient between the transmitting antenna and the active antenna for three location of the transistor (h_2=5mm, h_2=15mm and h_2=25mm). These results are plotted in Figure 8. The global shape of the $|S_{21}|$ for different transistor locations is well predicted and the theoretical results are in agreement with the measurements as a function of frequency From this results, at 130MHz, the measured transmission coefficient $|S_{21}|$ are close to-52dB and-48.17dB respectively for h_2=25mm and for h_2=5mm.

Location of the transistor	Simulated bandwidth (MHz)	Measured bandwidth (MHz)
h_2=25mm	69-162 (80%)	47-107 (78%)
h_2=15mm	70-165 (81%)	53-128 (83%)
h_2=5mm	78-190 (83%)	57-158 (94%)

Table 2. Simulated and measured bandwidth versus transistor location on the active antenna in common emitter configuration

http://dx.doi.org/10.5772/58839

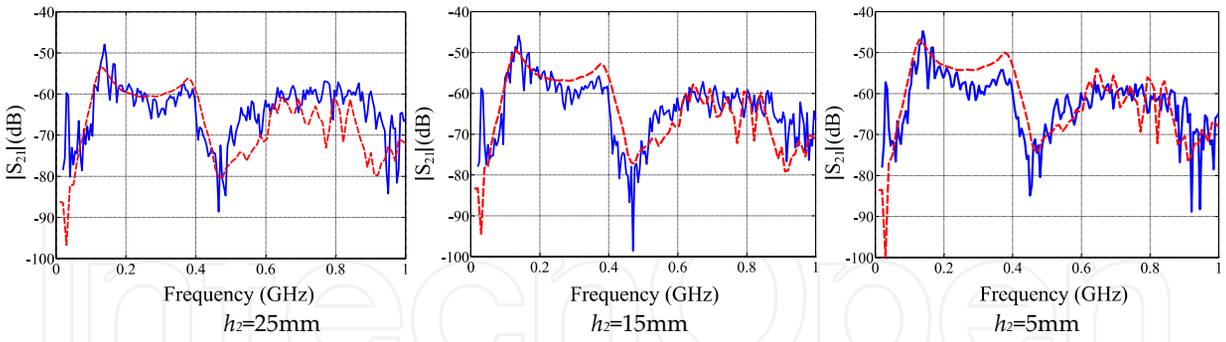

Figure 8. Transmission coefficients $|S_{21}|$ between reference antenna and active receiving antenna

From the FRIIS formula, we can estimate the measured and theoretical gain of the active receiving antenna at 130MHz. We measured a gain of-25.7dBi for h_1=25mm and-21.8dBi for h_2=5mm. The difference between these gains is closed to 3.9 dB and is due to the position of transistor on monopole. We notice that the highest gain is obtained when the transistor is very close from the ground plane (h_2=5mm). This gain level should be compared to the gain provided by an equivalent passive antenna with the same height (-49dBi).

b. Common collector configuration

In this second part, we present the same simulated and measured results of the active antenna as function of location of the transistor (h_2) for the common collector configuration. The results of $|S_{22}|$ are plotted in

Figure 9. There is a central resonance frequency around 100 MHz as in the common emitter configuration. Matching is always better in simulation and the bandwidth increases when the transistor is close to the reflector plane.

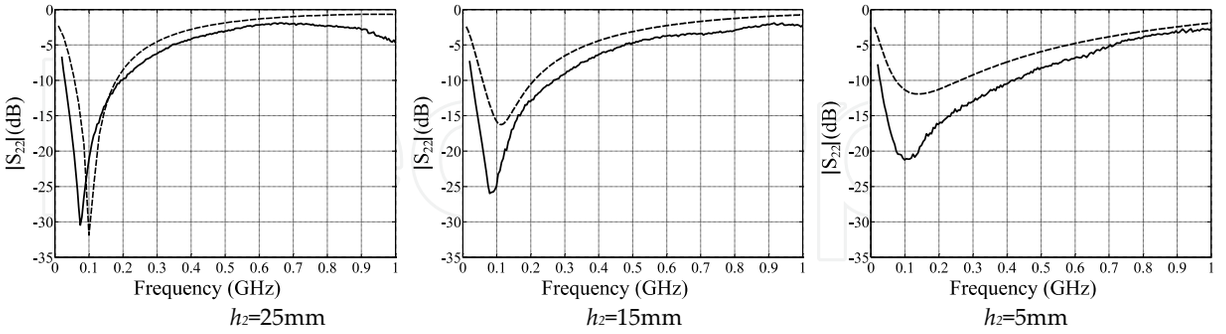

(—measurement,---simulation)

Figure 9. $|S_{22}|$ of the active receiving antenna in common collector configuration

We reported in the Table 3 the simulated and measured results.

Location of the transistor	Simulated bandwidth (MHz)	Measured bandwidth (MHz)
h_2=25mm	58-182 (103%)	29-198 (148%)
h_2=15mm	60-210 (111%)	28-272 (162%)
h_2=5mm	70-260 (115%)	27-426 (176%)

Table 3. Simulated and measured bandwidth versus transistor location on the active antenna in common collector configuration

Figure 10 presents the transmission coefficient $|S_{21}|$ as a function of the position of the transistor in common collector configuration for a height h_1=30mm. The results are presented from 50 MHz to 1 GHz frequency band to compare the behavior of the receiving active antenna as a function of frequency between simulations and measurements in order to validate the simulation methods. Agreements between the measured and simulated results are obtained. At 130 MHz, we obtained a transmission coefficient $|S_{21}|$ of-54.3 dB for a transistor positioned at h_2=25mm over to the reflector plane, of-53.8 dB for h_2=15mm and-53.8 dB when h_2=5mm.

Using the Friis formula, we calculates a gain of-28 dBi for the active receiving antenna when h_2=25mm and-27.58 dBi for h_2=5mm. The gain is almost identical between the two positions of the transistor.

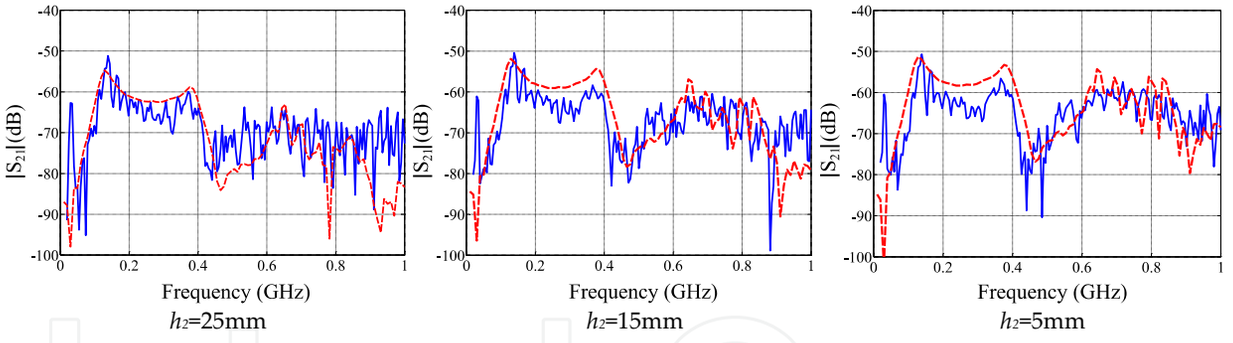

Figure 10. Transmission coefficients $|S_{21}|$ between reference antenna and active receiving antenna

These measurement results are very interesting towards the size and frequency bandwidth of the active receiving antenna and we underline that we can adjust the antenna bandwidth and the size reduction of the active receiving antenna compared to the wavelength by changing the position of the transistor.

2.4.2.2. Radiation patterns

To confirm our link budget calculation, we present in this part the measured radiation patterns of the active receiving antenna as function of the position of the transistor (h_2). We present the results of two heights h_2=25mm and h_2=5mm.

http://dx.doi.org/10.5772/58839

Figure 11 present the position of the active monopole over a reflector plane (500 mm x 500 mm) and the radiation pattern reference.

Figure 12 and Figure 13 show the radiation patterns of the active receiving monopole for both configurations, common emitter and common collector at several frequencies in FM band (88-108MHz). The radiation of the active antenna according to the frequency is similar to the radiation of a conventional monopole with vertical polarization.

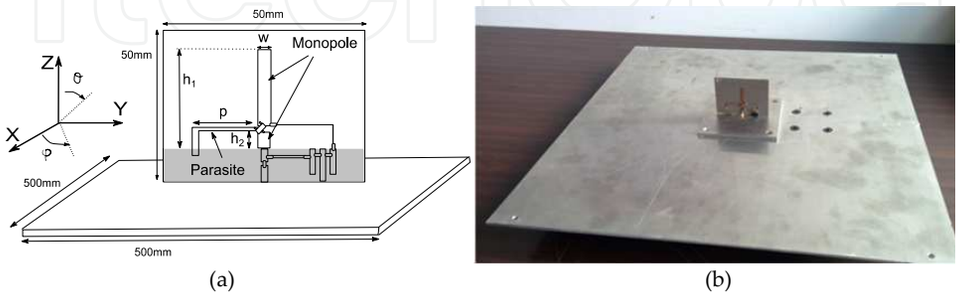

Figure 11. (a) Geometry of the antenna (b) Photography of the antenna prototype on the ground plane

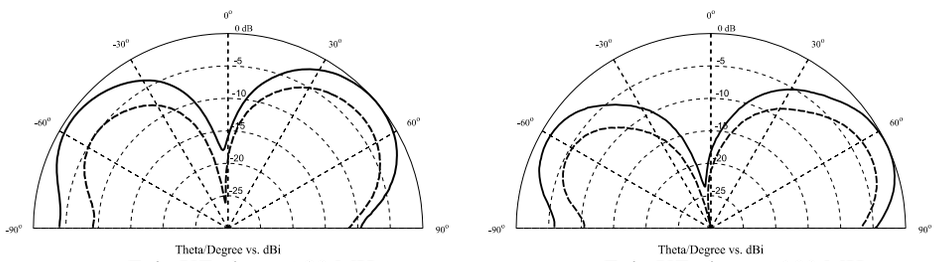

(—— h_2=5mm, h_2=25mm)

Figure 12. Normalized measured radiation patterns of the active receiving antenna in common emitter configuration

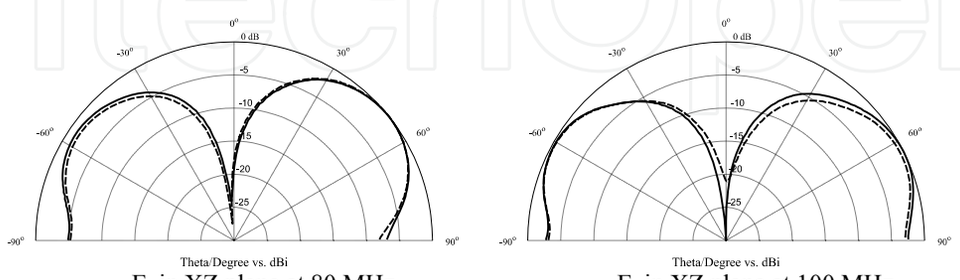

(—— h_2=5mm, h_2=25mm)

Figure 13. Normalized measured radiation patterns of the active receiving antenna in common collector configuration

As we have noticed above, the antenna gain depends on the transistor position. The gain variation between the two positions of the transistor is more important in common emitter than in common collector configuration. For example at 100 MHz, a gain of-22.6 dBi is measured for h_2=25mm and-19.6 dBi for h_2=5mm in common emitter configuration and-27.5 dBi for h_2=25mm and-27.3 dBi for h_2=5mm common collector configuration. Thus, there is a variation of 3 dB on common emitter and 0.2 dB common collector when h_2 varies from 25mm to 5mm.

The variations of transistor position provide the variation on the size reduction, bandwidth and the gain of active receiving antenna. The highest gain is obtained when the transistor is very close to the ground plane. For common emitter configuration, we have measured a gain of-19.6dBi at 100MHz and a bandwidth of 94% around 107.5MHz. In common collector configuration, the gain is equal to-27.3 dBi at 100MHz and the bandwidth is close to 176% around 226 MHz. The height of the active antenna is close to $\lambda/175$ and $\lambda/370$ in common emitter and common collector configuration respectively, where λ is the wavelength at the lowest operating frequency.

2.4.3. Influence of the position of the parasite

The study of active monopole is focused on two parameters: the height of the active receiving antenna (h_1) and the position of the transistor (h_2). In this part, the variation of the parasitic element position p is investigated (Figure 14). Indeed, the parasitic element is used to polarize the transistor and its length provides a variation of the input impedance of the active monopole.

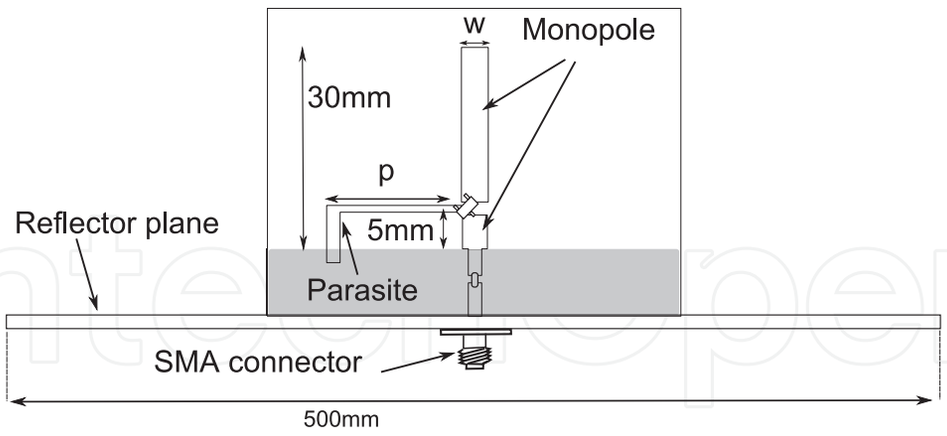

Figure 14. Position of the parasite in active antenna

2.4.3.1. Parametric studies

To observe the influence of the distance of (p) on the performances of the active antenna, this parameter has been sweep between 20 mm and 0.5 mm. The total length of the parasitic element varies from 25 mm to 5.5 mm. The simulation results of $|S_{11}|$ are shown in Figure 15.

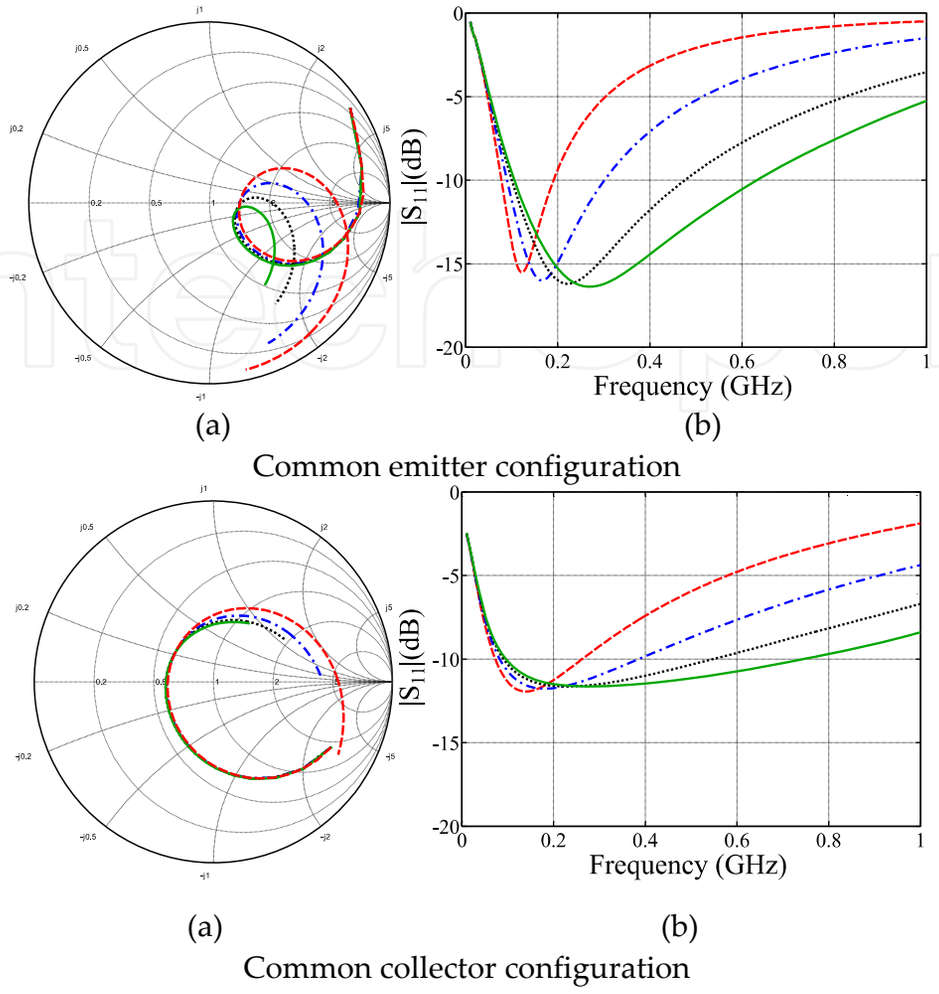

(——*p*=0.5mm, ⋯ *p*=5mm,-·-*p*=10mm,---*p*=20mm)

Figure 15. (a) Theoretical impedances of the active monopole as function of the position of the parasite *p* (b) Theoretical return loss active monopole based on the position of the parasite *p*.

It can be noticed that the bandwidth of the active antenna increases as *p* decreases, for the two configurations: common emitter and common collector. The results are summarized in Table 4.

Position of the parasite p (mm)	Bandwidth (MHz)	
	Common emitter	Common collector
20	78-190 (83%)	70-260 (115%)
10	90-300 (107%)	82-385 (130%)
5	100-474 (130%)	90-550 (143%)
0.5	105-632 (143%)	96-741 (154%)

Table 4. Simulated bandwidth versus parasite position (*p*) on the active antenna

2.4.3.2. Experimental results

To validate the theoretical studies of the influence of the position of the parasite on the impedance of the antenna, measurement results for two positions of the parasite in the common emitter and common collector configurations are presented. For the first one, p is equal to 20mm, for the second, p=0.5mm.

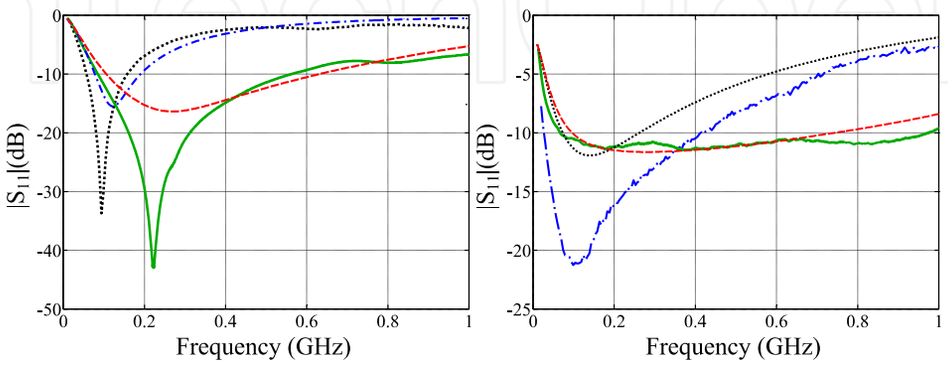

(—— measured p=0.5mm, ⋯ measured p=20mm,-·-·-simulated p=20mm,---simulated p=0.5mm)

Figure 16. Measured return loss of the active monopole antenna based on the position of the parasite p.

The variation of the parasitic element position can enhance the bandwidth of active receiving antenna as shown in Figure 16. For the common emitter configuration, we measured a bandwidth of 94% around 107 MHz for p=20 mm and a bandwidth of 149.5% around 320 MHz for p=0.5mm. For the common collector configuration, when p=0.5mm, there is a-10 dB bandwidth of 175% around 521 MHz measurement (Table 5). For the two configurations, the measurements and simulations are in good agreements.

	Emitter common configuration		Collector common configuration	
	Simulated	**Measured**	**Simulated**	**Measured**
p=20mm	78-190	57-158	70-260	27-426
p=0.5mm	105-636	81-560	96-741	65-978

Table 5. Simulated and measured bandwidth (MHz) versus parasite position (p) on the active antenna

2.4.4. Influence of the geometry of the monopole

In the first part of this chapter, we have presented the influence of different parameters on the performance of an active receiving monopole. The influence of the transistor position and the parasitic element position on the size reduction, on the bandwidth and on the gain has been clearly underlined.

http://dx.doi.org/10.5772/58839

To improve the gain performance of the active monopole antenna, we change the geometry of the antenna, especially on the upper part of the monopole. The transistor is in common emitter configuration positioned at h_2=5mm (h_1=30mm, p=0.5mm).

We calculated and measured two structures of active monopole antenna (Figure 17), the length of the upper part of the monopole ranges from 25 mm to 106 mm.

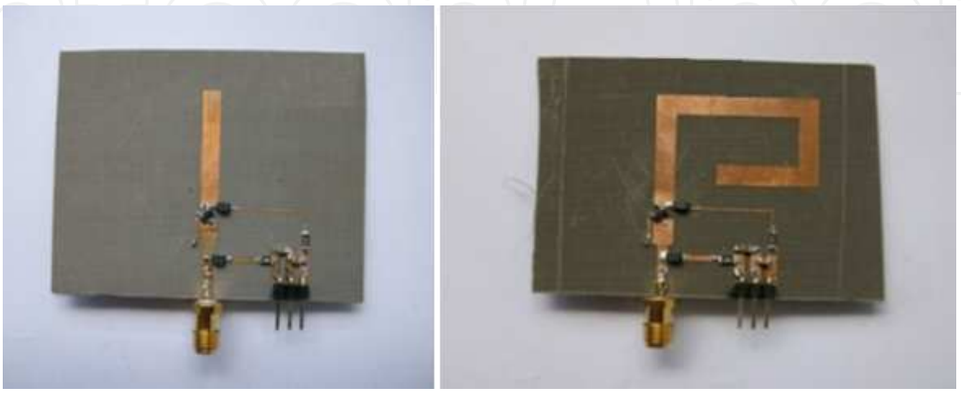

Figure 17. Geometry of the active monopole antenna

The theoretical and experimental return losses of the active antenna as a function of the length of the upper part of the monopole are presented in Figure 18.

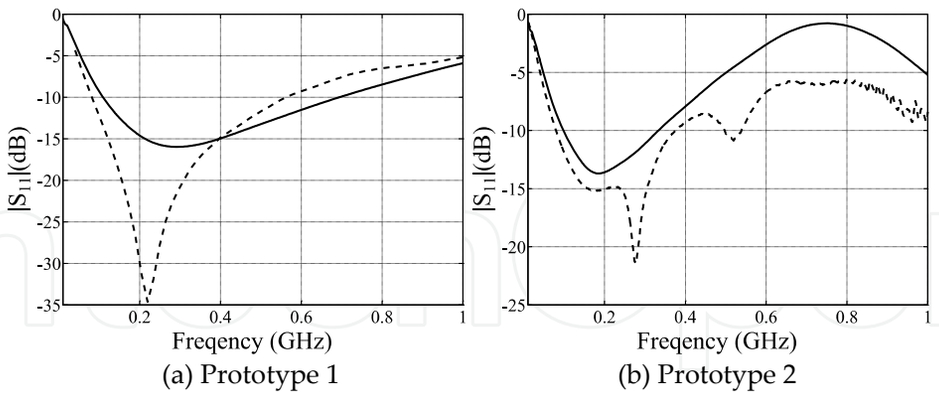

(---measured, —— simulated)

Figure 18. return losses of active monopole antenna

There is a frequency shift between measurements and simulations. However, measurements and simulations are in a good agreement. We measured a bandwidth of 150% around 322 MHz for prototype 1 and 130 % around 228 MHz for prototype 2. These results are summarized in Table 6.

	simulated BW (MHz)	measured BW (MHz)
Prototype 1	108-693 (146%)	81-563 (150%)
Prototype 2	97-335(110%)	80-377(130%)

Table 6. Simulated and measured bandwidth of the active antenna

In Figure 19, we presented the measured radiation patterns of the proposed antenna at 80 MHz and 100MHz. Radiation patterns are in good agreement for the bending structure and the classical one. A maximum gain of-21.57 dBi at 100 MHz was measured for the prototype 1 and-15.11 dBi for prototype 2. We have a difference of 6 dB between the two prototypes.

For evaluate the performances of active antenna in FM radio reception, we have measured the received signal strength indicator and the signal to noise ratio in FM band using the FM receiver evaluation board of silicon labs (Si4706).

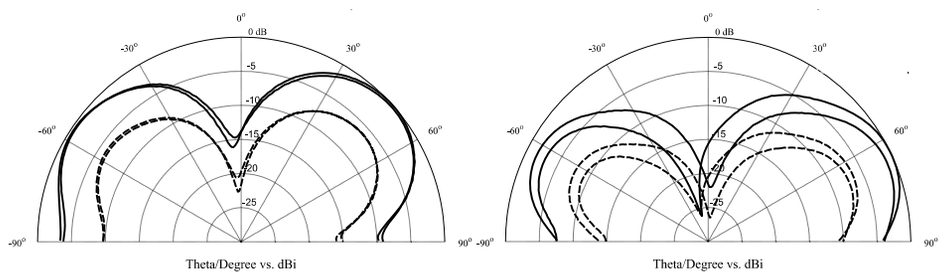

(---prototype 1, —— prototype 2)

Figure 19. Measured normalized radiation patterns of the active antenna in the XZ and YZ plan

The results are plotted for the active receiving antenna (prototype 2) and a reference monopole antenna of 60cm of height. The average power received by the reference $\lambda/4$ monopole antenna is 10dB higher than the power received by active receiving antenna. Despite the reduction of the power level, we measured a good received signal quality for listen to FM radio without interference.

2.5. Conclusion

In this first section, we studied the influence of the integration of a transistor on a passive monopole antenna, including the miniaturization of the antenna and the increase of the frequency bandwidth. Our contribution is based on the results obtained by Meinke in 60-70th and we conducted a theoretical and experimental validation of the active receiving antennas.

Despite the difficulty to simulate an active antenna, we use CST software to achieve consistency between measurements and simulations. Several parameters, as the position of the transistor, the position of the parasite and the design of the antenna are investigated.

http://dx.doi.org/10.5772/58839

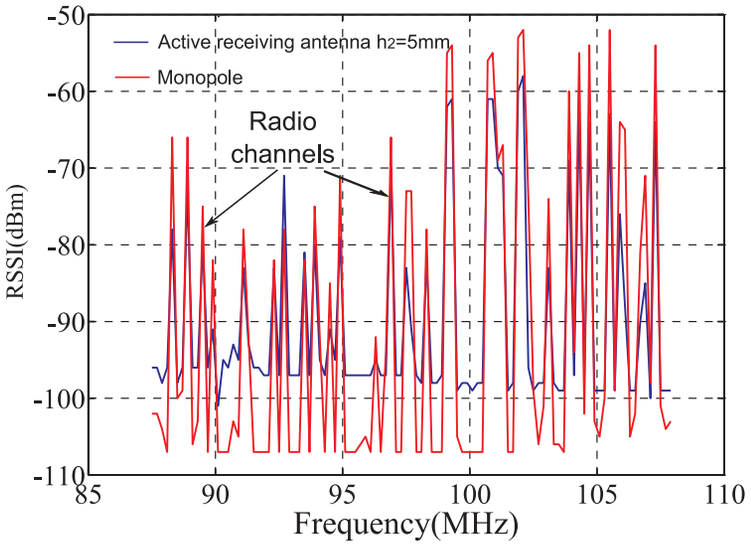

Figure 20. Received Signal Strength Indicator in FM band.

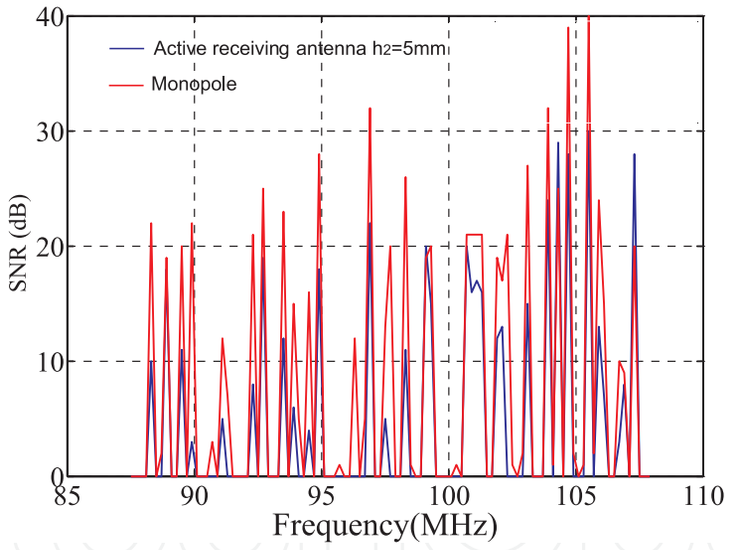

Figure 21. Signal to Noise Ratio

We also studied two configurations of transistor, i.e. common emitter and common collector. It was found that each configuration provides different performances. The bandwidth is wider in common collector (176%) than common emitter (94%). The reduction size is equal to $\lambda/370$ in common collector configuration and $\lambda/175$ in a common emitter.

Concerning the gain, the common emitter configuration presents a gain of-19.6 dBi which is higher than the gain (-27.3 dBi) obtained with the common collector configuration. These gains must be compared to gain a classical monopole of the same height (30mm) which is-49dBi.

Finally, the change of active monopole geometries has allowed us to increase the gain of the active antenna. It led to the creation of a miniature active antenna with a bandwidth of 130% around 228 MHz, the height of the active antenna is $\lambda/80$ at the lowest frequency of the bandwidth. The measured gain is-15.1 dBi at 100 MHz. We have measured a good received signal quality.

3. Compact tunable antenna

3.1. Introduction

Over the past years, efforts have been made to design small antennas in the UHF band for handset applications. Because of the convergent trend, limited space is available for each antenna device. For applications like broadcast reception, the antenna should be able to cover 40% of the relative bandwidth from 470 to 702 MHz. Regarding the wavelength at the lowest part of the bandwidth ($\lambda_{0=}$638 mm), it is obvious that small antennas are required for such applications.

To meet this requirement, the strategy is to cover the frequency range of such broadband applications using frequency tunable antennas. The basic antenna is then narrow band and the implementation of active devices introduces a frequency tunable ability. From a system point of view, it provides frequency selectable functions, which improve the signal-to-noise ratio. In [20-22], the authors show a compact tuned antenna for mobile applications. In [20,21], varactor diodes have been associated with PIFAs or meander antennas. Radiation patterns and S_{11} demonstrate the antenna's performances. In [23], an RF switch has been chosen rather than a varactor diode to avoid radiation influence on the device. The received measurement results show the validity of the concept.

In this section, we will consider the theoretical and physical aspects of self-inductance and investigate its effect on the resonance frequency of the MCLA (Monopole Coupled Loop Antenna) [24]. We studied them in order to explain the evolution of size reduction and the radiation pattern. We obtained a 55% reduction in the size of the antenna compared to the initial MCLA.

Finally, we associate a varactor diode with a small modified open-circuit MCLA in order to continuously control the frequency with a DC bias voltage. As a result a desirable frequency in a broadband frequency range covering 470–675 MHz is achieved. Experimental and theoretical results including S_{11}, radiation patterns and gain are in good agreement.

3.2. Monopole Coupled Loop Antenna (MCLA)

In this paragraph, we propose to feed a short circuited printed half loop antenna through an electromagnetic coupling using an arc monopole line [24]. The half loop, short circuited on its both sides, has been associated to an arc monopole fed by a 50Ω SMA connector as described in Figure 22. The antenna has been printed on a dielectric substrate circuit board and mounted above a finite reflector ground plane. The theoretical antenna performances have been

computed with CST Microwave Studio Software and compared to measurements. Regarding this first part of the study, we propose a physical explanation of the antenna behavior. Thereafter, parametric studies give additional information and help us to increase our knowledge of this design.

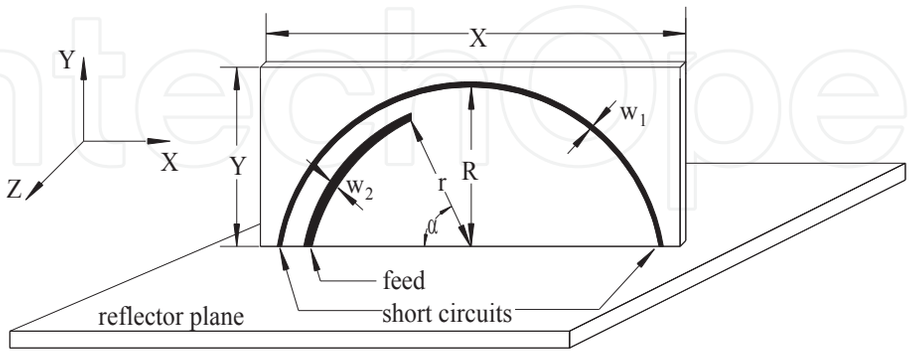

Figure 22. Geometry of the proposed antenna

R and r are respectively the radii of the half loop and the arc monopole lines, w_1 and w_2 are their widths. P is the total length of the arc monopole line and α is the angle between its both extremities. The radius (thus the length) of the half loop line will remain constant.

By an optimized choice of the lengths, the widths and the distance between the two lines, it is possible to achieve a broadband solution presented in Figure 23. The antenna has been printed on a Neltec NY9300 substrate (ε_r=3, h=0.786 mm, tanδ=0.0023) and above a limited square ground plane (300×300×4 mm^3).

In this case, R=100 mm, r=84 mm, w_1=0.4 mm, w_2=0.5 mm, X=220 mm, Y=110 mm, α=90° and P=132 mm. The return loss and the input impedance of the antenna have been computed. The simulation and measurement have been performed between 200MHz and 800MHz.

The Figure 23 shows a comparison between simulation and measurement with a very good agreement. The measured return loss bandwidth is close to 70MHz (≈15.3%). With this design, we increase three times the bandwidth of the antenna proposed in [25].

On Figure 23.a, the shape of the return loss shows two resonances. The first resonance frequency depends of the $\lambda/2$ half loop radiator, whereas the second one has been created by the arc monopole considered as a quarter wavelength conventional monopole. As noticed in reference [26], the electromagnetic coupling between the two parts of the antenna affects the impedance behavior.

To increase our understanding of this antenna, we proceed to theoretical parametric studies. We investigate the dimensions of the ground plane, the length, the width of the arc monopole line, the width of the half-loop line and the distance between the two microstrip lines and we will show the influence of these parameters on the input impedance. In this section, we present just two parameters, the length of the arc monopole and the distance between the two printed lines.

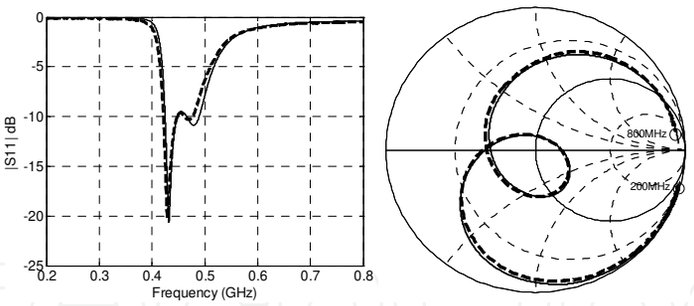

(a) (b)

(---) measured, (—) simulated

Figure 23. (a) Simulated and measured return losses for the MCLA, (b) Simulated and measured antenna input impedances

3.2.1. Length of the arc monopole

In Figure 24, we present the input impedance of the MCLA versus α which is the angle between the extremities of the arc monopole. α varies from 64.8° to 133°. We notice that there are no modifications on the other half loop parameters. The circles on the curves represent the resonance frequencies of the arc monopole (Figure 24).

The resonance of the half loop remains constant (Figure 23). The resonance mode of the arc monopole decreases when the length of this line increases. The best case is for α=90°, the resonance frequencies of the two lines are quite close and the impedance matching criterion S_{11} <-10 dB has been used to calculate the impedance bandwidth (70MHz or 15.3%). In the other case, the lower resonance frequency is too far from the highest one and it introduces a mismatching phenomenon. In Figure 24(a), for α=103.7°, both resonance frequencies are so close that they seem to be a single one. On Figure 24(b), we can distinguish these two resonances.

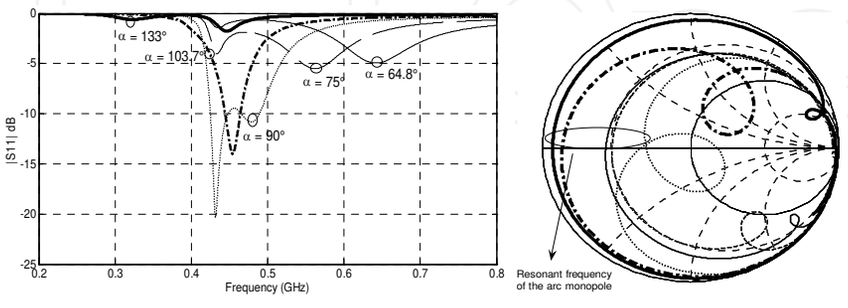

(a) (b)

(▬) α=133°, (- -) α=103.7°, (···) α=90°,(----) α=75°, (—) α=64.8°.

Figure 24. (a) Return losses of the simulated MCLA versus α (b) simulated MCLA input impedances, the frequency is varying between 200 and 800MHz.

3.2.2. Distance between the two printed lines

In Figure 25, three values of the arc monopole radius r have been used to characterize the MCLA. r varies from 70 mm to 95 mm and α is variable to keep the same length of the arc monopole. R=100 mm, w_1=0.4 mm, w_2=0.5 mm, P=132 mm, X=220 mm and Y=110 mm.

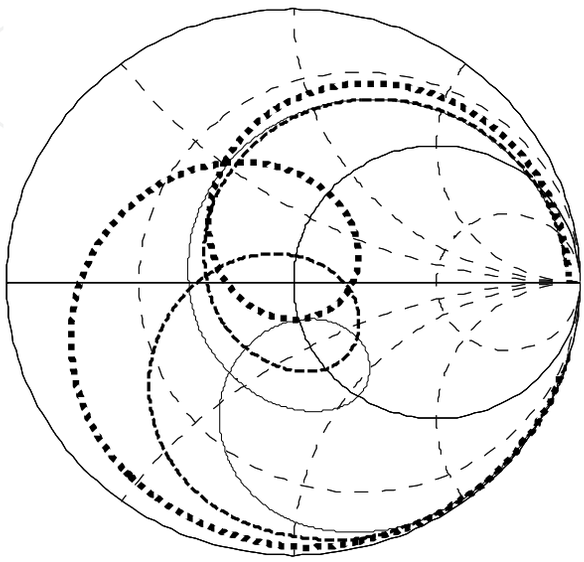

(—) r=70mm, (----) r=84mm, (···) r=95mm

Figure 25. Simulated MCLA input impedances when the radius of the arc loop is varying between 70mm and 95mm (the other parameters are constant), the frequency is varying between 200 and 800MHz.

The resonance frequency of the arc monopole decreases when the radius of this line increases. The best case is for r=84mm. These variations demonstrate that the coupling effect is very sensitive to the distance between the half loop and the arc monopole. The resonance of the half loop remains constant.

A monopole coupled loop antenna (MCLA) has been proposed [24]. A better impedance bandwidth has been obtained by electromagnetic coupling effect between the two microstrip lines (arc monopole+half loop). Its bandwidth is three times wider than the conventional half loop short circuited monopole [25]. In the next paragraph, different techniques will be used to reduce the size of the MCLA.

3.3. MCLA loaded by self-inductance

To achieve our first purpose (size reduction of the antenna), we modify the MCLA presented in previous paragraph by loading the short circuit of the half-loop on the left side with a self inductance (Figure 26). The ground plane is an infinite one [27].

The main dimensions of the antenna are listed below: R=100mm, r=84mm, w_1=0.4mm, w_2=0.5mm, Y=220mm, Z=110mm, α=90°.

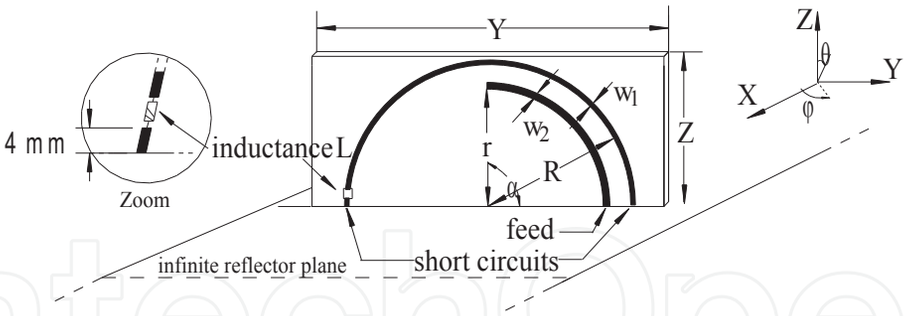

Figure 26. Geometry of the proposed antenna

The inductor component used below is an ATC 0805 WL modelled with a parallel RLC device. Simulations have been performed with CST Microwave studio® where the equivalent RLC circuit model has been introduced as lumped components [27].

In Figure 27, we present the input impedance of the MCLA loaded versus self inductance value. The self values vary from 0nH (equivalent to short circuit) to an infinite value (equivalent to an open circuit).

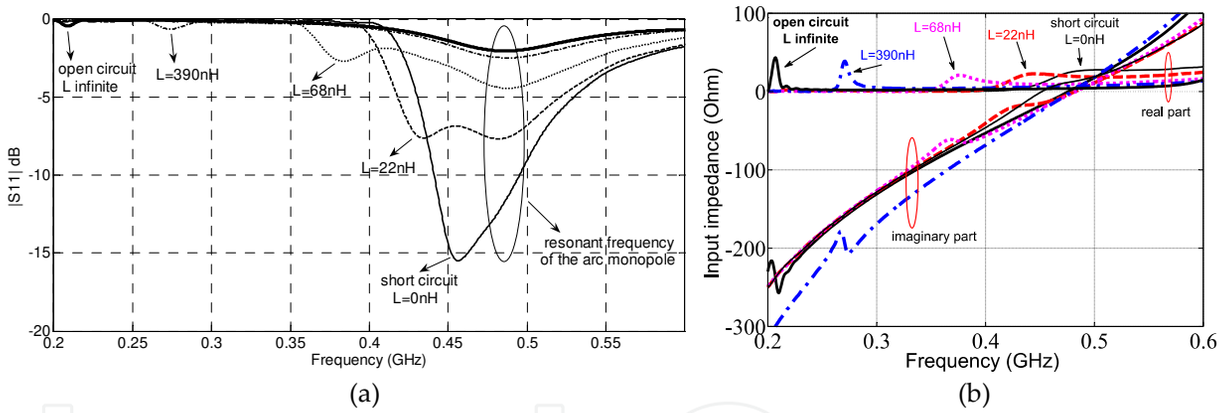

Figure 27. (a) Simulated return losses for the proposed antenna with different values of the self inductance, (b) Simulated input impedance for the proposed antenna with different values of the self inductance

In Figure 27, for each inductance, we can notice two resonance frequencies. The first one, linked to the arc monopole, remains constant and very close to 450MHz, whatever the self inductor values. The second one linked to the half loop radiator associated to the self inductor decreases from 455MHz to 209MHz. We can also notice that for these resonances, the antenna becomes more and more mismatched when the inductance value increases. In the previous paragraph we have mentioned that the antenna return losses at these resonance frequencies could be matched by modifying the length of the arc monopole.

To complete this calculation, we have computed and represented the normalized radiation patterns of the short circuited MCLA (L=0nH) (Figure 28).

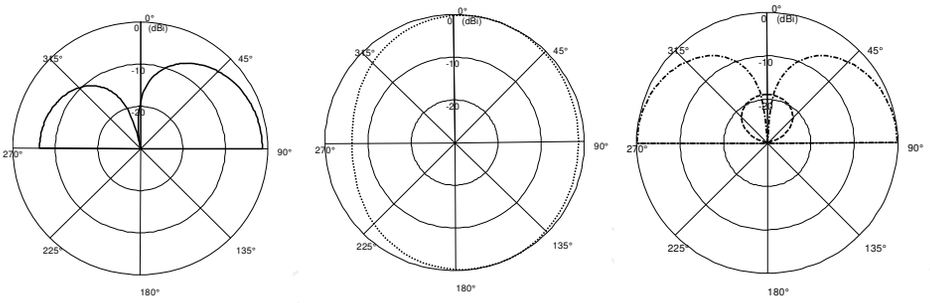

Figure 28. Normalized radiation patterns of the short circuited MCLA (L=0nH). (a) E_θ in YZ-plane φ=90°, (b) E_θ in XY-plane θ=90°, (c) (----) E_θ in XZ-plane and (- -) E_φ in XZ-plane φ=0°

For YZ-plane (Figure 28.a), we obtain a dissymmetric shape of radiation pattern due to the arc monopole influence [24]. In XY-plane, the radiation pattern is quasi-omnidirectional. Except the dissymmetry of the radiation pattern in YZ plane, we can notice that the general behavior of the antenna is very close to this provides by a monopole. The gain is equal to 1.8 dBi at 460 MHz.

This analysis is completed by drawing surface currents on the radiating elements (Figure 29).

Near to the feed point and to the short circuit areas, the surface currents are maximum. It explains that the maximum radiations are obtained for the E_θ in YZ-plane when θ=90°, and for the E_θ in XZ-plane when θ=90° or 270°. In Figure 29, the surface currents become null in z direction.

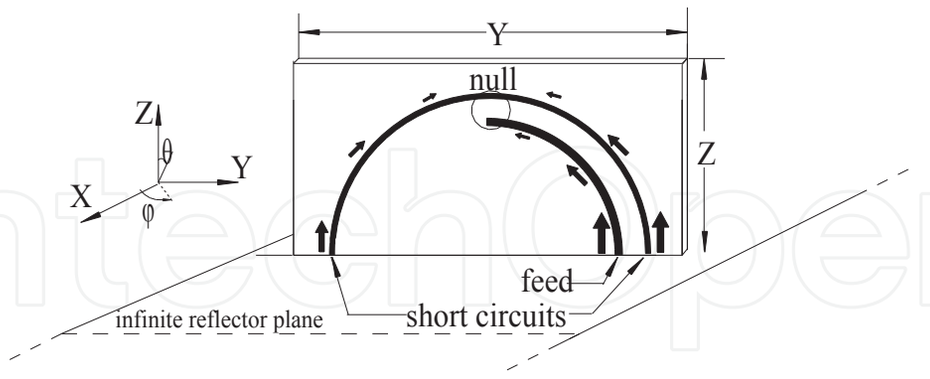

Figure 29. Schematic of surface currents distribution on radiator elements of short circuited MCLA

By increasing the value of the inductor, the deep null in the radiation pattern in YZ plane disappears and the antenna provides a quasi unidirectional pattern in this plane. This phenomenon could be explained in the Figure 30 where surface currents have been represented when the inductance value is 390 nH. Then, we notice that the half-loop surface currents distribution shifts to the left.

The inductance modifies the equivalent antenna electrical length and we can deduce that the antenna operating wavelength is lower than half a wavelength. In the extreme case, where the self inductance is infinite and equivalent to an open circuit, the open circuited MCLA operating wavelength becomes equal to a quarter wavelength.

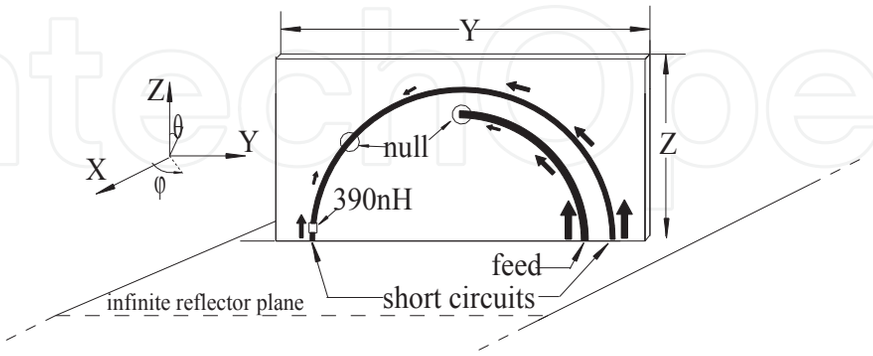

Figure 30. Schematic of surface currents distribution on elements of the MCLA loaded by a 390nH inductance

3.4. Modified open-circuit MCLA

We keep the case of the modified MCLA with an infinite self inductance [27]. We call this antenna modified open circuit MCLA. As mentioned in the previous paragraph and in [24], we could modify the arc monopole length to enhance the impedance bandwidth. As we wish that the antenna operates at 450MHz, we have optimized the arc monopole length to achieve both impedance matching and size reduction.

In Figure 31, we remind the modified open circuited MCLA design. For practical reasons, the antenna is placed perpendicularly above a limited square ground plane (300mm x 300mm x 4mm).

The main dimensions of the antenna are listed below: R=44.5mm, r=40.5mm, w_1=1mm, w_2=2mm, Y=100mm, Z=50mm, α=178.5°. The reduction size of the modified antenna is 55.5% compared to the initial MCLA.

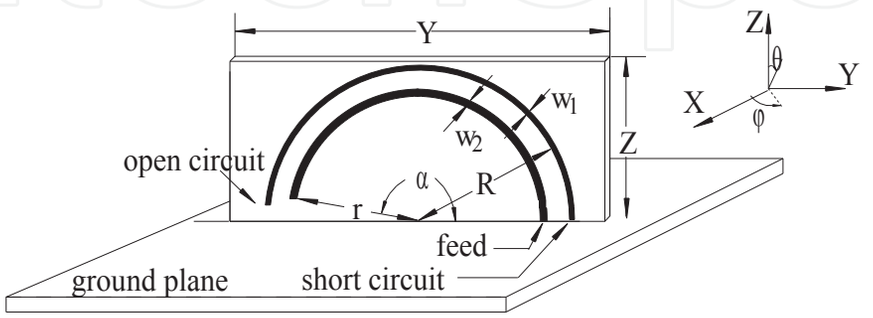

Figure 31. Geometry of the modified open circuited MCLA

The Figure 32 shows the theoretical and the measured return losses and input impedance with a good agreement.

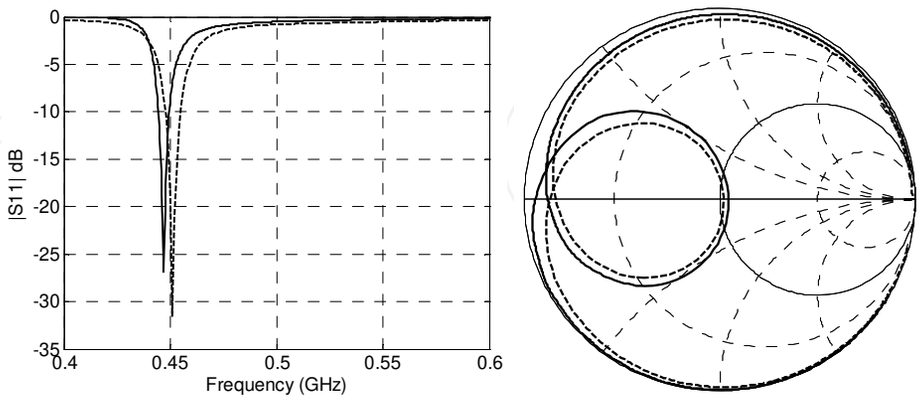

(a) (b)

(---) measured, (—) simulated

Figure 32. (a) Simulated and measured return losses for the modified open circuit MCLA (b) Simulated and measured antenna input impedances.

In Figure 33, we present the measured and simulated normalized radiation patterns of the modified open circuit MCLA.

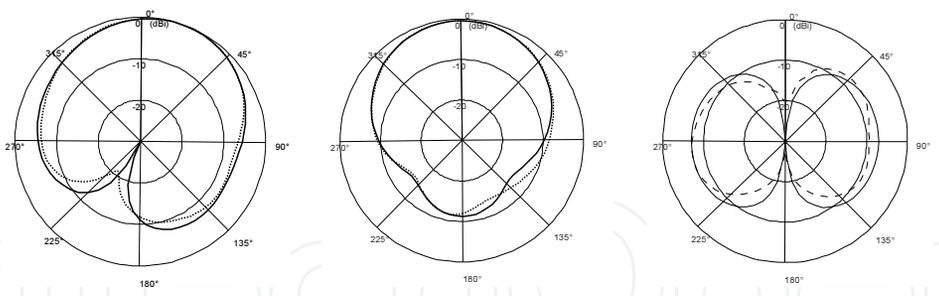

(---) measured, (—) simulated

Figure 33. Normalized radiation patterns at 448 MHz

As expected, the radiation pattern is quasi unidirectional and the agreement between theory and experience is good. At 448 MHz, the measured and the theoretical gain are respectively 3.8dBi and 3.9 dBi and the comparison is also good.

While the inductor element is well-known to decrease the antenna resonance frequency, based on MCLA, a theoretical study has been performed to demonstrate the modification of radiating behavior of MCLA loaded with inductance. Thus a modified open circuit MCLA has been

proposed. This antenna provides quasi unidirectional radiation pattern and size reduction (55.5%) compare to the initial MCLA [24]. The measured gain is high (3.8dBi).

3.5. Frequency tunable MCLA

In this section we present a frequency tunable antenna made with an open circuit Monopole Coupled Loop Antenna (MCLA) associated to a varactor diode [29]. The proposed antenna shows a 35,8% relative bandwidth, covering the [470-675]MHz frequency range.

We investigate the capability to obtain a frequency tunable antenna with reduced size open circuit MCLA. The antenna resonance frequency is controlled with a varactor diode fed having a DC bias voltage range of [0-5]V. This low voltage requirement made this diode suitable for handset application.

Performances of tunable antenna have been first investigated using CST® software, substituting the diode by its equivalent circuit. The varactor component used below is a MA4ST2200 from MACOM. The equivalent circuit proposed by the vendor is a series RLC circuit with a parallel capacitance (Figure 34). C_s is the tunable capacitor. The varactor has been characterized using a vector network analyzer and then the equivalent circuit has been obtained through a de-embedding process. In order to keep an operating frequency close to 470 MHz when the DC bias voltage is equal to zero, the parameters of the modified MCLA open circuit have been optimized with the corresponding diode equivalent circuit characteristics.

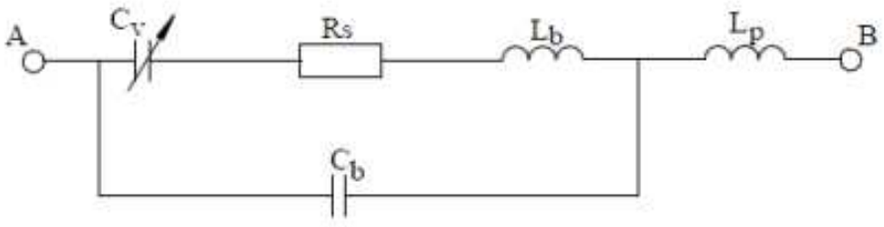

Figure 34. Equivalent circuit model of the varactor diode

A sketch of the prototype is reported in Figure 35, including the diode located on the short circuit side of the MCLA (right hand side of the drawing). The antenna has been printed on a Neltec NY9300 circuit board (ε_r=3, h=0.786 mm) and is placed perpendicularly to a square ground plane (300 mm x 300 mm x 4 mm). R and r are the radius of the half loop and the arc monopole lines respectively, w_1 and w_2 are their widths. α is the angle between the arc monopole extremities. The main dimensions of the antenna are listed below: R=37.5 mm, r=34.5 mm, w_1=1 mm, w_2=2 mm, Y=80 mm, Z=40 mm, α=43.5°.

The bias circuit used to carry a DC control voltage to the varactor without interfering with the high frequency currents is reported in Figure 35. In order to isolate the DC voltage from RF signal a choke L=2200 nH, a series resistance 5 kΩ and one chip capacitor (5 nF) are used.

http://dx.doi.org/10.5772/58839

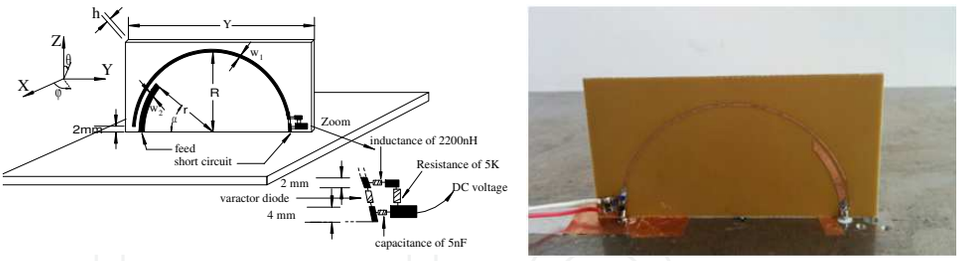

(a) (b)

Figure 35. (a) Geometry of the open circuit MCLA (b) Photography of the antenna prototype

Antenna performances for different DC control voltage values obtained with CST software have been compared to measurement results. In Figure 36, good agreement between simulated and measured return loss for a few voltage values can be seen.

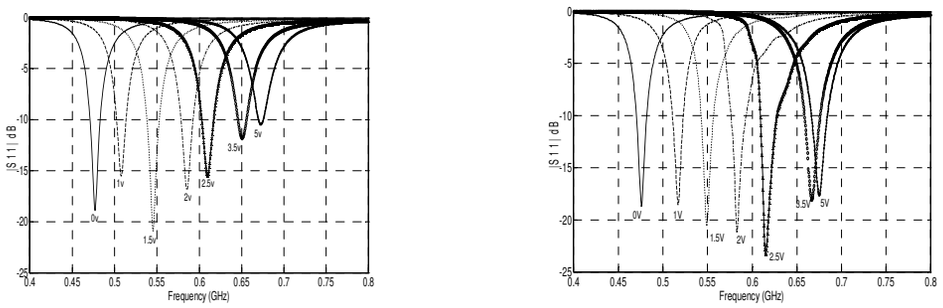

(a) (b)

Figure 36. (a) Simulated and (b) measured return losses

As depicted in Figure 36, the antenna covers the [470-675] MHz frequency range, which corresponds to a 35,8% relative-10dB adaptation bandwidth. For each resonance, the corresponding instantaneous bandwidth is more than 10MHz.

Normalized radiation patterns comparison for the frequency range extrema values 474MHz and 668MHz, corresponding to 0V and 5V DC order, show as well acceptable agreement. It has to be noticed that the behavior of the antenna radiation patterns in the main planes (YZ and XZ planes) is quasi unidirectional in the entire band. The cross-polarization in the XZ-plane becomes very low when the resonance frequency increases. The front to back radiation level decreases when the resonance frequency increases.

Good agreement is obtained for simulated and measured maximum gains versus operating frequencies (Figure 37). It has to be underlined that considering the antenna electrical dimensions ($\lambda/17 \times \lambda/8$ at 470MHz), a high gain on the whole frequency range is provided, and especially in the higher band.

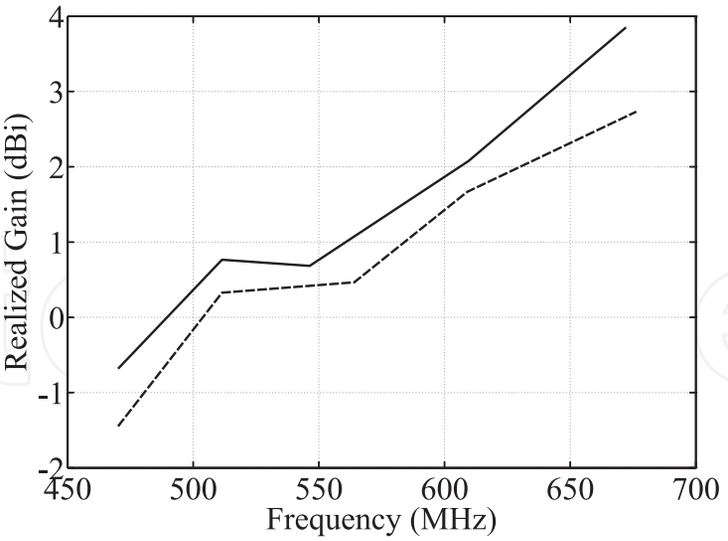

(---) measured (—) simulated

Figure 37. Simulated and measured maximum gains

3.6. Conclusion

A varactor-tuned open circuit MCLA has been designed and realized. The aim of this study is to provide a simple technique to sweep the instantaneous bandwidth of the structure from 470 MHz to 675 MHz. The measured maximum gain varies between-1.5dBi to 2.8dBi. In future, this antenna can be miniaturized in order to be included in a terminal mobile. Theoretical and experimental results of S_{11}, radiation patterns and gain have been performed and show good agreement.

3.7. General conclusion

The objectives of this chapter concern the design and the development of compact active antennas, working on a wide frequency band. We have presented innovative techniques to reduce the antenna size with a wide cover frequency rang. We have demonstrated two solutions; the first one is broadband antenna with very important size reduction and wide bandwidth. The second one is a tunable antenna.

In the first part, the capabilities offered by active antennas for miniaturization by the integration of actives components directly on the antenna have been presented and their impact on printed antenna's performances (bandwidth, size reduction, and gain) investigated theoretically and experimentally. Regarding the small volume dedicated for antenna in devices, a broadband miniature active antenna operating in the FM band has been presented.

In the second section, a technique of narrowband antennas miniaturization for DVB-H applications has been proposed. Some new designs of miniaturized antennas based on a coupling feeding system have been proposed and fabricated. Thus, these antennas have been associated with varactor diodes in order to achieve frequency tunable antenna.

Author details

Y. Taachouche, M. Abdallah, F. Colombel, G. Le Ray and M. Himdi*

*Address all correspondence to: mohamed.himdi@univ-rennes1.fr

Institute of Electronic and Telecommunication of Rennes (IETR), University of Rennes , Rennes, France

References

[1] H. A. Wheeler, 'Fundamental limitations of small antennas', Proc. IRE, 35, pp. 1479-1484, Dec. 1947.

[2] H. A. Wheeler, "Small Antennas" IEEE Trans. Antennas Propagat., vol. 23, pp. 462-469, July 1975.

[3] Jenshan. Lin, Itoh, T, "Active Integrated Antennas", Microwave Theory and Techniques, IEEE Transactions on, vol. 42, issue 12, pp. 2186-2194, Dec 1994.

[4] H.H. Meinke. "Transistorized receiving antennas" Institut fur Hochfrequenztechnik der Technischen Hochschule, Munchen, November 1967, 99 pages.

[5] J. R. Copeland, W. J. Robertson, R. J. Verstraete, "Antennafier arrays", Antennas and Propagation, IEEE Transactions on, vol 12, Issue 2, pp. 227-233, Mar 1964.

[6] F. M. Landstorfer, H. H. Meinke, "Transistorized Microwave Antenna with 1GHz Centre frequency", Microwave Conference, 2nd European, vol 1, pp.1-4, 1971.

[7] Anderson. A, Davies. W, Dawoud. M, Galanakis. D, " Note on Transistor-Fed Active-Array Antennas", Antennas and Propagation, IEEE Transactions on, vol 19, Issue 4, pp. 537-539, 1971.

[8] Ramsdale. P.A, MacLean. T. S. M, "Active Loop-Dipole Aerials", Electrical Engineers, Proceedings of the Institution of, vol 119, issue 4, pp 423-424, 1972.

[9] Rangole. P.K, Saini. S.P.S, "Transistor Configurations in Integrated Transistor Antennas", Radio and Electronic Engineer, vol 45, issue 3, 1975.

[10] Ramsdale. P.A, MacLean. T.S.M, "Active Loop-Dipole Aerials", Electrical Engineers, Proceedings of the Institution of, vol 118, issue 12, pp. 1698-1710, 1971.

[11] Rangole. P.K, Midha. S.S, "Short antenna with active inductance", Electronics Letters, vol 10, issue 22, pp. 462-463, 1974.

[12] Y. Qian, Tatsuo Itoh, "Progress in active integrated antennas and their applications" IEEE transactions on microwave theory and technique, Vol. 46, No. 11, Nov 1998, pp. 1891-1900.

[13] T.S.M MacLean and G. Marris, "Short rang active transmitting antenna with very large height reduction". IEEE. Transactions on antennas and propagation. March 1975, pp. 286-287.

[14] A.P.Anderson, M. Dawoud, "The performance of transistor fed monopoles in active antennas" IEEE transactions on antennas and propagation, Vol:21, issue:3, may 1973, pp. 371-374.

[15] V. B. Ertürk, R. G. Rojas, and P. Roblin, "Hybrid analysis/design method for active integrated antennas," IEE Proc.-Microw. Antennas Propagat., vol. 146, pp. 131-137,1999.

[16] P.S. Hall, "Analysis of radiation from active microstrip antennas" Electronics letters, 7th january 1993, vol 29, n°1, pp. 127-129.

[17] H. An, B. K. J. C. Nauwelaers, A. R. Van de Capelle, R. G. Bosisio, "A novel measurement technique for amplifier-type active antennas". Microwave symposium digest, IEEE MTT-S international. 1994, Vol3, pp. 1473-1476.

[18] Taachouche, Y.; Colombel, F.; Himdi, M., "Influence of the transistor location on the behavior of a transistorized printed antenna," *Antennas and Propagation (EUCAP), 2012 6th European Conference on,* vol., no., pp.1255,1258, 26-30 March 2012

[19] Y. Taachouche, F. Colombel, and M. Himdi, "Very Compact and Broadband Active Antenna for VHF Band Applications," International Journal of Antennas and Propagation, vol. 2012, Article ID 193716, 4 pages, 2012

[20] Nguyen, V.-A., Dao, M.-T., Lim, Y.T., and Park, S.-O.: 'A compact tunable internal antenna for personal communication handsets', IEEE Antennas Wire. Propag. Lett., 2008, 7, pp. 569–572

[21] Komulainen, M., Berg, M., Jantunen, H., and Salonen, E.: 'Compact varactor-tuned meander line monopole antenna for DVB-H signal reception', Electron. Lett., 2007, 43, (24), pp. 1324–1326

[22] Yoon, I.-J., Park, S.-H., and Kim, Y.-E.: 'Frequency tunable antenna for mobile TV signal reception'. IEEE AP-S Int. Symp. Dig., 2007, pp. 5861–5864

[23] Suzuki, H., Ohba, I., and Minemura, T.: 'Frequency tunable antennas for mobile phone for terrestrial digital TV broadcasting reception'. IEEE AP-S Int. Symp. Dig., Singapore, 2006, pp. 2329–2332.

[24] Abdallah, M.; Colombel, F.; Le Ray, G.; Himdi, M., "Novel Printed Monopole Coupled Loop Antenna," *Antennas and Wireless Propagation Letters, IEEE*, vol.7, no., pp. 221,224, 2008.

[25] H. Lebbar, "Analyse et conception d'antennes imprimées multifilaires", phd thesis, University of Rennes 1, France, october 1994.

[26] Z. N. Chen and Y.W.M. Chia, 'Broadband monopole antenna with parasitic planar element', Microwave Opt. Technol. Lett., Vol.27, No. 3, pp. 209-210, Nov. 2000.

[27] Abdallah, M.; Colombel, F.; Le Ray, G.; Himdi, M., "Quasi-Unidirectional Radiation Pattern of Monopole Coupled Loop Antenna," *Antennas and Wireless Propagation Letters, IEEE*, vol.8, no., pp.732,735, 2009.

[28] Taachouche, Y.; Colombel, F.; Himdi, M., "Meandered monopole coupled loop antenna," *Antennas and Propagation (EUCAP), 2012 6th European Conference on*, vol., no., pp. 3005,3008, 26-30 March 2012.

[29] Abdallah, M.; Le Coq, L.; Colombel, F.; Le Ray, G.; Himdi, M., "Frequency tunable monopole coupled loop antenna with broadside radiation pattern," *Electronics Letters*, vol.45, no.23, pp.1149,1151, November 2009.

IntechOpen

IntechOpen

IntechOpen